Aluminum Conducts Better than Copper at the Atomic Scale: A First-Principles Study of Metallic Atomic Wires

Adam J. Simbeck,[†,∥,*] Nick Lanzillo,[†,∥] Neerav Kharche,[†,‡] Matthieu J. Verstraete,[§] and Saroj K. Nayak[†]

[†]Department of Physics, Applied Physics, and Astronomy and [‡]Computational Center for Nanotechnology Innovations, Rensselaer Polytechnic Institute, Troy, New York 12180, United States, and [§]Nanomat Unit, Department of Physics, University of Liege, B-4000 Liege, Belgium. [∥]Co-first authors.

ABSTRACT Using a first-principles density functional method, we have studied the electronic structure, electron−phonon coupling, and quantum transport properties of atomic wires of Ag, Al, Au, and Cu. Non-equilibrium Green's function-based transport studies of finite atomic wires suggest that the conductivity of Al atomic wires is higher than that of Ag, Au, and Cu in contrast to the bulk where Al has the lowest conductivity among these systems. This is attributed to the higher number of eigenchannels in Al wires, which becomes the determining factor in the ballistic limit. On the basis of density functional perturbation theory, we find that the electron−phonon coupling constant of the Al atomic wire is lowest among the four metals studied, and more importantly, that the value is reduced by a factor of 50 compared to the bulk.

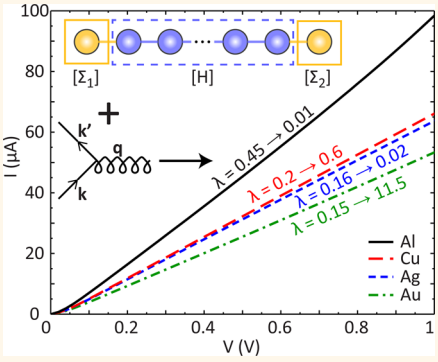

KEYWORDS: metallic atomic wires · ballistic quantum transport · electron−phonon coupling · Eliashberg theory

It is no surprise that the well-defined properties of a bulk material do not necessarily carry over to the nanoscale. Rather, it has been shown both theoretically[1] and experimentally[1,2] that such a transition results in a number of new and interesting phenomena. Over the past decade, one area that has received significant attention within the context of quantum confinement is the study of linear chains of metallic atoms (*i.e.*, metallic nanowires).[1−20] One striking result from this research is the Landauer formalism, which states that the conductance in nanoscale systems is quantized in units of $G_0 = 2e^2/h$, where e is the fundamental unit of charge and h is Planck's constant.[21] Experimentally, quantized conductance has been verified in a number of nanoscale systems[1,2] and also spurred a number of innovations in scanning tunneling microscopy (STM) and mechanical controllable break junction (MCBJ) techniques.[15] Even more interesting is the behavior of such systems as a function of width and under stress and strain. It has been shown both experimentally[22] and theoretically[18] that such extreme confinement results in oscillations in the conductance as a function of the wire length. Furthermore, it has been demonstrated that the behavior of an atomic-sized contact under stress and strain is largely dependent upon the atomic species.[8,19] As for application purposes, metallic nanowires are a key area of research since they represent the ultimate miniaturization of conductors, that is, the manipulation of individual atoms. More specifically, the evolution of the conductance as a function of nanowire cross-sectional area as the dimensions of chip components, such as Cu interconnects, approach the mean free path of the electron (~40 nm) is of great interest.

Despite the efforts mentioned above, the specific question posed by the title of this paper "Does aluminum conduct better than copper at the atomic scale?" appears to be one area that has received less attention[3,4,23] over the same time period. Scheer *et al.* studied the conductance properties of different atomic wires experimentally and conjectured that the number of current-carrying channels, or eigenchannels, is determined

* Address correspondence to simbea@rpi.edu.

Received for review August 28, 2012 and accepted October 19, 2012.

Published online October 19, 2012
10.1021/nn303950b

by the valence state of the respective atom.[3] Building off of this general reasoning, Hasmy *et al.* used semiclassical molecular dynamics simulations to study Al nanocontacts, where it was reported that the conductance for such systems converged to a value between G_0 and $1.5G_0$.[4] Hasmy *et al.* then concluded that Al nanocontacts are, per atom, better conductors than any monovalent metal. Again, this argument is based on the *rule of thumb* from ref 3. A similar trend was reported by Kapur *et al.* when comparing the theoretical resistivity *versus* wire cross-section curves for Cu and Al interconnects.[23] This study was based on both empirical relations and the bulk resistivity values of Cu and Al. It was found that the slopes of such curves indicated that, as compared to Cu, the effects of surface and grain boundary scattering being less in Al may eventually lead to lower resistivity in Al compared with Cu.

Although refs 3, 4, and 22 have laid the groundwork for the question we pose, an unambiguous answer remains elusive. In order to address this question, an atomic-level analysis of the conductivity of different metal wires, where both contacts and nanowires are treated at the quantum mechanical level, is required. In this study, our aim is to not only compare the conductance properties of Al atomic wires to those composed of noble metals but also to include the effects of electron−phonon (e−ph) interactions such that we may demonstrate further benefits of Al at such small length scales. Scattering mechanisms in such devices have been considered in other works. For example, the effect of scattering due to transition metal impurities in Cu nanowires has been theoretically shown to reduce conductance.[17] Furthermore, e−ph interactions in metallic nanowires have also been investigated, but the majority of the research done thus far focuses on finite Au wires and, in particular, the effect of phonon emission on the conductance.[24−26] In addition, the explicit treatment of e−ph coupling *via* Eliashberg theory has only been treated for Al and Pb atomic wires[27] and for Na wires.[28] To date, no comparison of e−ph interactions in Al the noble metals has been made. In addition, the fundamental understanding of the modified e−ph coupling in nanowires has not been addressed. Such interactions are particularly interesting for applications of nanowires as interconnects in integrated circuits since a dominant contribution to the conductivity of metals comes from e−ph coupling.

In this paper, we present electronic structure, ballistic quantum transport properties, and e−ph coupling for atomic wires of Al, Ag, Au, and Cu. The electronic structure analysis is based on a first-principles density functional method; the e−ph coupling is computed within the scheme of density functional perturbation theory (DFPT), and the quantum transport properties are computed using a non-equilibrium Green's function (NEGF) formalism. More specifically, we are interested in how the contact affects quantum transport in atomic wires of different materials, as well as how the e−ph coupling changes when going from the bulk to the extreme case of atomic wires. In this study, we treat Ag, Al, Au, and Cu atomic wires by first considering wires of finite length (1−3 nm) attached to Au contacts. Here we perform quantum transport calculations to compute low bias (up to 1.0 V) current *versus* voltage (*IV*) curves as well as density of states (DOS). We find that even with the presence of the contact the current through the Al atomic wire is higher than that of Ag, Au, and Cu. While the ballistic limit results are encouraging, one would also like to understand how the conductivity of these atomic wires compares when the length of the wire exceeds the mean free path of the electron. Here infinite, one-dimensional (1D) atomic wires are sufficient to study such an effect. Therefore, our transport results are further corroborated by an analysis of the band structures of 1D metallic atomic wires. Finally, we perform calculations of the e−ph coupling constant λ in 1D Ag, Al, Au, and Cu atomic wires following the scheme of refs 27, 29, and 30. As compared to the bulk, we report a decrease in the e−ph coupling constant for Al by a factor of 50. We also report a reduction in the coupling constant for Ag, although the change is not as high as in the case of Al, while for Au and Cu, an enhancement in λ, relative to the bulk, is predicted. Such results are understood by changes in bond length and interatomic force constants, as well as the *l*, *m* character of the electronic states which couple to phonons.

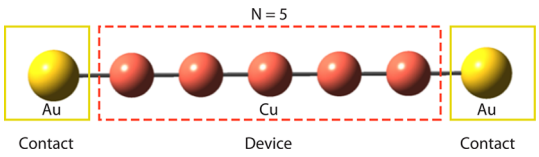

Figure 1. Arrangement of the linear, finite metallic atomic wire systems. The device consists of *N* = 3−10 (1−3 nm) metallic atoms whose interatomic separations are chosen to match optimized separations in 1D chains. The contacts are taken as single Au atoms. The example shown is for *N* = 5 Cu.

RESULTS AND DISCUSSION

Finite Chains. For the sake of simplicity, the geometries considered for the quantum transport calculations under the Landauer formalism were linear, nonperiodic *N* atom chains, where *N* = 3−10 (Figure 1). The interatomic separations were chosen to match the optimized separations in 1D chains found using the ABINIT density functional theory (DFT) package (see results for 1D chains below). These *N* atom chains define our atomic wire device. Since only a few of the essentially infinite number of atoms in the contact will influence the atomic wire, we take the contacts as single Au atoms, where again the separation between

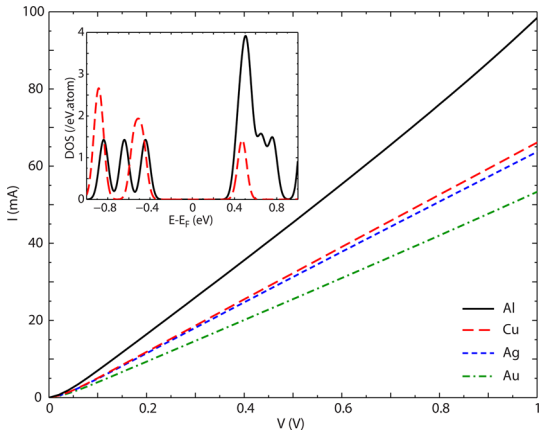

Figure 2. Current *vs* voltage (*IV*) plots for $N = 5$ metallic atomic wires. Note the increased current seen in the Al case (solid, black line), especially for larger (1.0 V) bias. The inset shows that the density of states (DOS) near the Fermi energy E_F is higher for the Al atomic wire as compared to Cu.

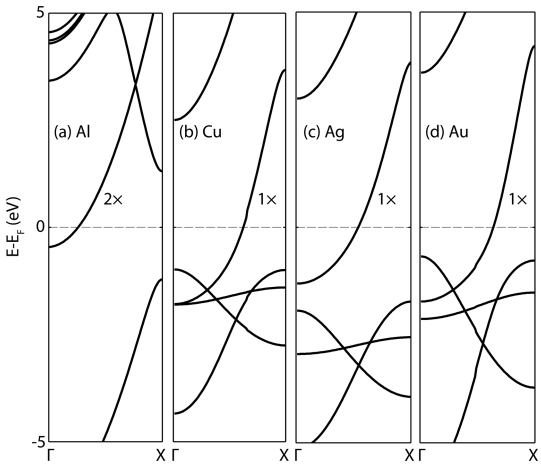

Figure 3. Band structures for 1D metallic atomic wires. All figures show one band crossing the Fermi energy E_F (dashed line), but the (a) Al band is two-fold degenerate.

contact and device was chosen to match the optimized Au interatomic spacing from the infinite wires. It was found that the use of larger contacts (20 Au atoms per contact) had no appreciable effect on the quantum transport results (see Methods and Supporting Information).

For the finite metallic atomic wires, the *IV* results from our NEGF quantum transport calculations are plotted in Figure 2. The transport calculation shows that at low bias (V < 1.0 V) the Al atomic wire conducts better than any of the other metals. This trend was confirmed for all wire sizes, such as $N = 3-10$, and can be understood by the rule of thumb from ref 3 or examining the DOS (Figure 2 inset), which clearly shows more states near the Fermi energy E_F for the Al system, as compared to Cu. The Ag and Au DOS are not featured in this inset because the results are similar to that of Cu; that is, the DOS near E_F is less than that of Al. From a mathematical point of view, these results are consistent because the higher DOS in the Al wire is reflected in a higher transmission (see Methods, eq 2), which in turn leads to greater current (see Methods, eq 1). We reiterate here that the contact size has negligible effects on our results. While the finite wire results are interesting, it is necessary to study the conductivity of such systems when the wire length exceeds the mean free path of the electron.

One-Dimensional Chains. For the 1D systems, the optimized separations from DFT were as follows: Ag 2.58 Å, Al 2.30 Å, Au 2.54 Å, and Cu 2.25 Å. The electronic band structure calculations (Figure 3) verify that in the ballistic limit, and for low bias, one should expect Al to conduct better than Ag, Au, or Cu. This is because the number of eigenchannels available for conduction in a 1D wire is determined by the number of bands crossing E_F (note that the Al band is two-fold degenerate).[17] Figure 3 is in excellent agreement with ref 12 for Al, Ag, and Au and ref 13 for Cu. Next, in order to move outside the ballistic regime, we also consider e−ph interactions.

The results of our e−ph coupling calculations within the framework of DFPT are presented in Figure 4 and Table 1. The e−ph coupling constant λ, which is a measure of the strength of interaction between electrons and phonons, is computed from a weighted integral over frequency (see Methods, eq 3) of the Eliashberg spectral function (A2F), which is a phonon density of states weighted according to interactions with electrons. The phonon band structure and e−ph coupling in each wire are very different from the bulk. In particular, the coupling constant of Al drops to 0.01. Ag sees a much smaller decrease. Cu and Au, on the other hand, both show increased coupling relative to the bulk. We note that all wires show a two-fold degenerate imaginary frequency transverse mode, which is a general feature of any 1D wire. For Al and Ag, the electrons do not couple to these modes but rather to the real longitudinal phonons (Figure 4a,b). At their respective equilibrium interatomic distances, both Cu and Au couple primarily to the imaginary frequency transverse mode (Figure 4c,e). This results in large coupling constants of around 0.4 due to the small absolute values of the frequencies of these modes. Note that similar coupling is seen for Pb wires in ref 25. By stretching the Cu and Au wires by 10 and 9% respectively, the phonon spectra become strictly positive and the electrons couple only to real-frequency phonon modes (Figure 4d,f). The values of λ are increased due to the presence of low-frequency phonon modes of less than 2 THz with which the electrons couple (Table 1). The drastic decrease in the overall coupling of Al is attributed to the shift in phonon frequencies (Figure 4a). The wire shows phonons close to 20 THz, compared with only 10 THz in the bulk.[30] Since the integral for the coupling constant goes as $1/\omega$ (see Methods, eq 3), these high-frequency contributions are effectively damped and the overall

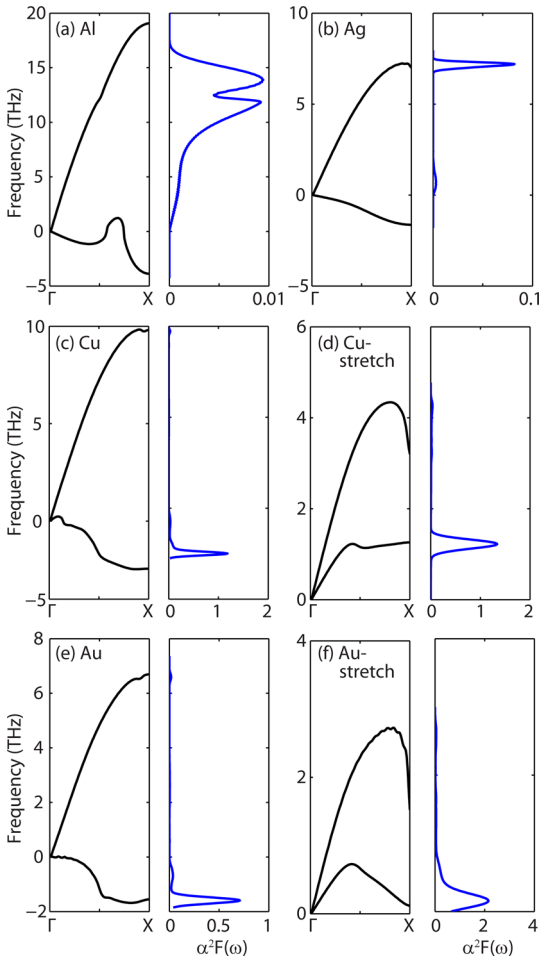

Figure 4. Phonon band structures and Eliashberg spectral functions $\alpha^2F(\omega)$. At the atomic scale, negative frequency modes occur for all four metals, but electrons only couple to these transverse modes in the cases of (c) Cu and (e) Au. Such negative frequency modes can be made positive by stretching, as in (d) Cu and (f) Au.

TABLE 1. Electron–Phonon Coupling Factor λ[a]

metal	λ_{bulk}	$\lambda_{atomic\ scale}$
Al	0.45	0.01
Ag	0.16	0.02
Au	0.2	11.5
Cu	0.15	0.6

[a] The results shown for Au and Cu atomic wires are for the stretched case.

coupling is very small. This raises the question of why Al sees such a large shift in phonon frequencies relative to the other metals. We first note that each metal shows phonon hardening relative to the bulk, but for Al, this change is more pronounced. We attribute this to the small bond length in the Al wire (2.30 Å), which is roughly half an angstrom smaller than the bulk nearest-neighbor separation. In the past, it has been reported that stretching an atomic wire results in smaller phonon frequencies,[31,32] and likewise, bringing atoms closer together should produce harder phonon modes. However, a microscopic understanding of this observation is not available. An analysis of the interatomic force constants (IFCs) along the direction of the wire reveals that the effective IFC per unit mass is largest for Al, followed by Cu, and finally by Ag and Au. This corresponds to the ordering of the maximum phonon frequency at the zone boundary for each wire. These effective force constants include up to seventh nearest-neighbor interactions. The IFCs for the Al wire also decay more slowly than in the other three wires, further contributing to the hardening of the phonon modes and reduction in λ.

These changes can be further understood in terms of a simple 1D model of a linear chain with nearest-neighbor interactions. If we take the effective IFCs obtained from DFPT and calculate the zone boundary ($k = \pi/a$) phonon frequency according to

$$\omega(k) = 2\sqrt{\frac{K_{eff}}{M}}\sin\left(\frac{ka}{2}\right)$$

we recover frequencies that agree with the explicit phonon band structures. For example, this calculation gives a phonon frequency of 18.4 THz for Al and 10.1 THz for Cu in the unstretched case. This validates the notion that the hardening of phonon frequencies at the atomic scale results from changes in the IFCs per unit mass, which are greater than those in the bulk.

Recent IETS experiments[24,25] have shown that for seven-atom Au chains, electrons couple to a longitudinal phonon with a frequency of 15 meV. A similar experiment for a short Al chain[33] shows electrons coupling to a transverse phonon with a frequency of 11 meV. Using Gaussian 03, we have confirmed that, for very short finite wires, such as those considered in the IETS experiments, the phonon frequencies differ from those found in a much longer wire. The results for the short wires though are in excellent agreement with experiment. For a seven-atom Au atomic wire, we find a longitudinal phonon with an unscaled frequency of 14.3 meV, while for a four-atom Al atomic wire, we find a transverse phonon with an unscaled frequency of 9.1 meV. These agree very well with the results of the IETS experiments. We expect that as longer wires become more tractable experimentally the trends will match those reported for our 1D atomic wires.

Finally, we would like to briefly mention that a connection can be drawn between the character of the states near the Fermi energy and the phonon modes to which electrons couple. The projected density of states (PDOS) for the Ag, Au, and Cu atomic wires has already been studied in ref 34. Here it is shown that, whereas the Au and Cu PDOS are dominated by states which have d-like character near the Fermi energy, the Ag PDOS has mainly s character. An analysis of the PDOS for Al (not shown here) reveals strong p character around the Fermi energy. For the Cu and Au atomic wire cases, it can be shown analytically that the d states

couple to transverse phonons, giving a large contribution to the overall e−ph coupling. Such d states appear near the Fermi energy due to confinement, in agreement with earlier experimental and computational studies of a Cu monatomic wire on a Pt substrate.[35] For the Al and Ag wires, however, the states near the Fermi level are p-like and s-like, respectively, and couple to longitudinal phonons. The longitudinal modes are at a higher frequency than the transverse modes and give a smaller contribution to the overall coupling. A simple tight binding model for a 1D atomic chain that takes into account the *l*, *m* decomposition of the electronic wave function, that is, is able to differentiate between s-, p-, and d-like orbitals, agrees with our detailed first-principles calculations presented above.[36]

CONCLUSION

In summary, we have studied the electronic structure of atomic wires of Ag, Al, Au, and Cu using first-principles electronic structure calculations.We find that in the ballistic limit Al conducts better than Ag, Au, or Cu even in the presence of the contact interfaces. The increase in conductivity of Al compared to other metals is ascribed to the higher number of channels near the Fermi energy available for transport. The results are extended to 1D atomic wires with similar trends. Interestingly, confinement also drastically modifies the e−ph coupling constant λ. In particular, λ for the Al wire is lowered by a factor of 50 (∼2% of bulk value). Other than Al, only Ag also shows a reduction in λ (∼13% of bulk value), whereas Au and Cu both show enhancements relative to the bulk. The change in e−ph coupling is related to hardening and softening of phonon modes in the atomic wires which results from changes in the atomic separation and likewise changes in the IFCs. This analysis is further supported by correlating the PDOS near the Fermi energy to the s, p, or d character of electrons which couple to specific phonon modes. Such results show promise for metallic nanowires as a segue from current Cu-based technology to the designs of the future.

METHODS

Finite Chains. The electronic structure density functional theory (DFT) calculations for quantum transport employed the Gaussian '03 (G03) ab initio quantum chemistry code.[37] We have used the Becke,[38] three-parameter, Lee−Yang−Par[39] (B3LYP) exchange-correlation energy functional and the LANL2DZ basis set, in which the Hay−Wadt[40] relativistic effective core potential (RECP) is employed. With G03 providing the energy and overlap matrices, quantum transport calculations for the ballistic system could be performed using the Green's function-based method of the Landauer formalism, which is outlined in ref 20. Essentially, current flows as a result of a difference between the Fermi distribution functions $f(E,\mu_1)$, $f(E,\mu_2)$ of the contacts

$$I = \left(\frac{e}{h}\right)\int T(E,V)[f(E,\mu_1) - f(E,\mu_2)]\mathrm{d}E \qquad (1)$$

where e is the fundamental charge, h is Planck's constant, T is the transmission probability, $\mu_{1,2}$ are the electrochemical potentials of the contacts, E is the energy of the injected electron, and V is the applied voltage. Note that the transmission function $T(E,V)$ is determined from the Green's function G

$$T = Tr[\Gamma_1 G \Gamma_2 G^{\dagger}] \qquad (2)$$

where $\Gamma_{1,2}$ describes the broadening and shift of the energy levels due to coupling with the contact. Here we point out that the inclusion of the single Au atom contacts (Figure 1) is necessary to explicitly calculate the coupling matrix between the contact and the device. The coupling matrices then allow for the evaluation of the self-energy matrices of the contacts, which describe the effects of the contacts on the device. The surface Green's function of each contact is also needed to derive the self-energy matrices. We have approximated the surface Green's function as a diagonal matrix with each element proportional to the local density of states of the s band of gold (0.035 per electron spin), which dominates the density of states near the Fermi energy. Similar approximations have been invoked in other works involving transport calculations.[41,42] It is also important to note that it was found that the modification of the electronic energy levels under bias is negligible and is therefore ignored in the transport calculations. For example, the inclusion of an external field of ∼0.002 au, which corresponds to a bias of 1.00 V, shifts the electronic energy levels involved in transport by less than 0.1 eV (see Supporting Information). A similar behavior in the electronic energy levels of the device under an applied bias has been noted in refs 42 and 43.

One-Dimensional Chains. For the 1D metallic atomic wires, the ABINIT code[44−47] was used for both the electronic as well as phononic calculations. For the atomic wires, 30 Bohr of vacuum in directions perpendicular to the longitudinal axis was used to ensure adjacent supercells did not interact. As a check of the optimized interatomic separations, two separate LDA pseudopotentials were also tested. For all cases, agreement to within 0.1 Å of the optimized interatomic spacing was found. For the 1D electronic band structure, a 1 × 1 × 256 k-point grid was used.

The e−ph coupling constant λ was also calculated for the 1D atomic wires described above. These computations were carried out within the framework of density functional perturbation theory (DFPT) in the ABINIT code. A plane wave cutoff of 10 Ha was used for Al and a cutoff of 40 Ha for Ag, Au, and Cu. All bulk simulations employed a 16 × 16 × 16 k-point grid and 8 × 8 × 8 q-point grid. Our computed electronic and phononic band structures agree with previous works.[30,48] The k-point and q-point grids for the atomic wires were 1 × 1 × 128 and 1 × 1 × 64, respectively. We note that our calculated quantities for Al agree with refs 27, 29, and 31.

The quantity λ, also known as the electron mass renormalization factor, is a measure of the scattering strength between electrons and phonons. In brief, the e−ph coupling constant is determined from the following integral over frequency ω

$$\lambda = 2\int_{\omega_{\min}}^{\infty} \frac{\alpha^2F(\omega)}{|\omega|}\,\mathrm{d}\omega \qquad (3)$$

where the quantity $\alpha^2F(\omega)$ is the Eliashberg spectral function (A2F), which is a phonon density of states weighted according to interactions with electrons.[28] Symbolically, α is the e−ph coupling strength in the Fröhlich Hamiltonian, and F refers to the phonon density of states. The integral runs from the minimum phonon frequency of A2F and sets the lower bound for the e−ph coupling constant integration. The relevant link between A2F and experiment is discussed in ref 49. For a more detailed outline of the calculation, we refer the reader to refs 27, 29, and 50.

Conflict of Interest: The authors declare no competing financial interest.

Acknowledgment. This work is supported by the Interconnect Focus Center (MARCO program), State of New York, the National Science Foundation (NSF) Integrative Graduate Education and Research Traineeship (IGERT) program, Grant No. 0333314, and the Communauté française de Belgique, through ARC grant "TheMoTherm" No. 10/15-03 and FRFC grant "Control of attosecond dynamics" No. 2.4545.12. Computing resources of the Computational Center for Nanotechnology Innovations (CCNI) at Rensselaer, partly funded by the State of New York, have been used for this work.

Supporting Information Available: Electric field effect on the energy levels of the channel and contact size effect in quantum transport calculations. This material is available free of charge *via* the Internet at http://pubs.acs.org.

REFERENCES AND NOTES

1. Scheer, E.; Joyez, P.; Esteve, D.; Urbina, C.; Devoret, M. H. Conduction Channel Transmissions of Atomic-Size Aluminum Contacts. *Phys. Rev. Lett.* **1997**, *78*, 3535–3538.
2. Ohnishi, H.; Kondo, Y.; Takayanagi, K. Quantized Conductance through Individual Rows of Suspended Gold Atoms. *Nature* **1998**, *395*, 780–783.
3. Scheer, E.; Agrait, N.; Cuevas, J. C.; Yeyati, A. L.; Ludoph, B.; Martin-Rodero, A.; Bollinger, G. R.; van Ruitenbeek, J. M.; Urbina, C. The Signature of Chemical Valence in the Electrical Conduction through a Single-Atom Contact. *Nature* **1998**, *394*, 154–157.
4. Hasmy, A.; Perez-Jimenez, A. J.; Palacios, J. J.; Garcia-Mochales, P.; Costa-Kramer, J. L.; Diaz, M.; Medina, E.; Serena, P. A. Ballistic Resistivity in Aluminum Nanocontacts. *Phys. Rev. B* **2005**, *72*, 245405.
5. Kobayashi, N.; Brandbyge, M.; Tsukada, M. First-Principles Study of Electron Transport through Monatomic Al and Na Wires. *Phys. Rev. B* **2000**, *62*, 8430–8437.
6. Brandbyge, M.; Sorensen, M. R.; Jacobsen, K. W. Conductance Eigenchannels in Nanocontacts. *Phys. Rev. B* **1997**, *56*, 14956–14959.
7. Cuevas, J. C.; Levy Yeyati, A.; Martin-Rodero, A. Microscopic Origin of Conducting Channels in Metallic Atomic-Size Contacts. *Phys. Rev. Lett.* **1998**, *80*, 1066–1069.
8. Cuevas, J. C.; Levy Yeyati, A.; Martin-Rodero, A.; Bollinger, G. R.; Untiedt, C.; Agrait, N. Evolution of Conducting Channels in Metallic Atomic Contacts under Elastic Deformation. *Phys. Rev. Lett.* **1998**, *81*, 2990–2993.
9. Mozos, J. L.; Ordejon, P.; Brandbyge, M.; Taylor, J.; Stokbro, K. Simulations of Quantum Transport in Nanoscale Systems: Application to Atomic Gold and Silver Wires. *Nanotechnology* **2002**, *13*, 346–351.
10. Brandbyge, M.; Kobayashi, N.; Tsukada, M. Conduction Channels at Finite Bias in Single-Atom Gold Contacts. *Phys. Rev. B* **1999**, *60*, 17064–17070.
11. Rodrigues, V.; Fuhrer, T.; Ugarte, D. Signature of Atomic Structure in the Quantum Conductance of Gold Nanowires. *Phys. Rev. Lett.* **2000**, *85*, 4124–4127.
12. Ribeiro, F. J.; Cohen, M. L. *Ab Initio* Pseudopotential Calculations of Infinite Monatomic Chains of Au, Al, Ag, Pd, Rh, and Ru. *Phys. Rev. B* **2003**, *68*, 035423.
13. Sanchez-Portal, D.; Artacho, E.; Junquera, J.; Garcia, A.; Soler, J. M. Zigzag Equilibrium Structure in Monatomic Wires. *Surf. Sci.* **2001**, *482*, 1261–1265.
14. Pascual, J. I.; Mendez, J.; Gomezherrero, J.; Baro, A. M.; Garcia, N.; Landman, U.; Luedtke, W. D.; Bogachek, E. N.; Cheng, H. P. Properties of Metallic Nanowires—From Conductance Quantization to Localization. *Science* **1995**, *267*, 1793–1795.
15. Costa-Kramer, J. L.; Garcia, N.; Garcia-Mochales, P.; Serena, P. A.; Marques, M. I.; Correia, A. Conductance Quantization in Nanowires Formed between Micro and Macroscopic Metallic Electrodes. *Phys. Rev. B* **1997**, *55*, 5416–5424.
16. Yanson, A. I.; Bollinger, G. R.; van den Brom, H. E.; Agrait, N.; van Ruitenbeek, J. M. Formation and Manipulation of a Metallic Wire of Single Gold Atoms. *Nature* **1998**, *395*, 783–785.
17. Papanikolaou, N.; Opitz, J.; Zahn, P.; Mertig, I. Spin-Filter Effect in Metallic Nanowires. *Phys. Rev. B* **2002**, *66*, 165441.
18. Thygesen, K. S.; Jacobsen, K. W. Four-Atom Period in the Conductance of Monatomic Al Wires. *Phys. Rev. Lett.* **2003**, *91*, 146801.
19. Sanchez-Portal, D.; Untiedt, C.; Soler, J. M.; Saenz, J. J.; Agrait, N. Nanocontacts: Probing Electronic Structure under Extreme Uniaxial Strains. *Phys. Rev. Lett.* **1997**, *79*, 4198–4201.
20. Mehrez, H.; Ciraci, S. Yielding and Fracture Mechanisms of Nanowires. *Phys. Rev. B* **1997**, *56*, 12632–12642.
21. Datta, S. *Quantum Transport: Atom to Transistor*; Cambridge University Press: Cambridge, UK, 2005.
22. Smit, R. H. M.; Untiedt, C.; Rubio-Bollinger, G.; Segers, R. C.; van Ruitenbeek, J. M. Observation of a Parity Oscillation in the Conductance of Atomic Wires. *Phys. Rev. Lett.* **2003**, *91*, 076805.
23. Kapur, P.; McVittie, J. P.; Saraswat, K. C. Technology and Reliability Constrained Future Copper Interconnects—Part I: Resistance Modeling. *IEEE Trans. Electron Devices* **2002**, *49*, 590–597.
24. Agrait, N.; Untiedt, C.; Rubio-Bollinger, G.; Vieira, S. Electron Transport and Phonons in Atomic Wires. *Chem. Phys.* **2002**, *281*, 231–234.
25. de la Vega, L.; Martin-Rodero, A.; Agrait, N.; Levy Yeyati, A. Universal Features of Electron−Phonon Interactions in Atomic Wires. *Phys. Rev. B* **2006**, *73*, 075428.
26. Agrait, N.; Untiedt, C.; Rubio-Bollinger, G.; Vieira, S. Onset of Energy Dissipation in Ballistic Atomic Wires. *Phys. Rev. Lett.* **2002**, *88*, 216803.
27. Verstraete, M. J.; Gonze, X. Phonon Band Structure and Electron−Phonon Interactions in Metallic Nanowires. *Phys. Rev. B* **2006**, *74*, 153408.
28. Sen, P. Peierls Instability and Electron−Phonon Coupling in a One-Dimensional Sodium Wire. *Chem. Phys. Lett.* **2006**, *428*, 430–435.
29. Verstraete, M. Ab Initio Calculations of the Structural, Electronic, and Superconducting Properties of Carbon Nanotubes and Nanowires, Universite Catholique de Louvain, Belgium, 2005.
30. Bauer, R.; Schmid, A.; Pavone, P.; Strauch, D. Electron−Phonon Coupling in the Metallic Elements Al, Au, Na, and Nb: A First-Principles Study. *Phys. Rev. B* **1998**, *57*, 11276–11282.
31. Picaud, F.; Dal Corso, A.; Tosatti, E. Phonons Softening in Tip-Stretched Monatomic Nanowires. *Surf. Sci.* **2003**, *532*, 544–548.
32. Frederiksen, T.; Paulsson, M.; Brandbyge, M.; Jauho, A. P. Inelastic Transport Theory from First Principles: Methodology and Application to Nanoscale Devices. *Phys. Rev. B* **2007**, *75*, 205413.
33. Bohler, T.; Edtbauer, A.; Scheer, E. Point-Contact Spectroscopy on Aluminium Atomic-Size Contacts: Longitudinal and Transverse Vibronic Excitations. *New J. Phys.* **2009**, *11*, 013036.
34. Zarechnaya, E. Y.; Skorodumova, N. V.; Simak, S. I.; Johansson, B.; Isaev, E. I. Theoretical Study of Linear Monoatomic Nanowires, Dimer and Bulk of Cu, Ag, Au, Ni, Pd and Pt. *Comput. Mater. Sci.* **2008**, *43*, 522–530.
35. Zhou, P. H.; Moras, P.; Ferrari, L.; Bihlmayer, G.; Blugel, S.; Carbone, C. One-Dimensional 3D Electronic Bands of Monatomic Cu Chains. *Phys. Rev. Lett.* **2008**, *101*, 036807.
36. Verstraete, M. J.; Lanzillo, N.; Simbeck, A. J.; Nayak, S. K. Combined First-Principles and Tight Binding Analysis of Electron-Phonon Interactions in Metallic Atomic Wires. To be published.
37. Frisch, M. J.; Trucks, G. W.; Schlegel, H. B.; Scuseria, G. E.; Robb, M. A.; Cheeseman, J. R.; Montgomery, J. A.; Vreven, T.; Kudin, K. N.; Burant, J. C.; *et al. Gaussain 03*, revision c.02 code; Gaussian, Inc.: Wallingford, CT, 2003.
38. Becke, A. D. Density-Functional Thermochemistry. III. The Role of Exact Exchange. *J. Chem. Phys.* **1993**, *98*, 5648–5652.

39. Lee, C. T.; Yang, W. T.; Parr, R. G. Development of the Colle-Salvetti Correlation-Energy Formula into a Functional of the Electron-Density. *Phys. Rev. B* **1988**, *37*, 785–789.
40. Hay, P. J.; Wadt, W. R. *Ab Initio* Effective Core Potentials for Molecular Calculations—Potentials for the Transition-Metal Atoms Sc to Hg. *J. Chem. Phys.* **1985**, *82*, 270–283.
41. Pati, R.; Mailman, M.; Senapati, L.; Ajayan, P. M.; Mahanti, S. D.; Nayak, S. K. Oscillatory Spin-Polarized Conductance in Carbon Atom Wires. *Phys. Rev. B* **2003**, *68*, 014412.
42. Pati, R.; Senapati, L.; Ajayan, P. M.; Nayak, S. K. First-Principles Calculations of Spin-Polarized Electron Transport in a Molecular Wire: Molecular Spin Valve. *Phys. Rev. B* **2003**, *68*, 100407.
43. Heurich, J.; Cuevas, J. C.; Wenzel, W.; Schon, G. Electrical Transport through Single-Molecule Junctions: From Molecular Orbitals to Conduction Channels. *Phys. Rev. Lett.* **2002**, *88*, 256803.
44. *ABINIT code*, Universit Catholique de Louvain and other contributers.
45. Gonze, X. First-Principles Responses of Solids to Atomic Displacements and Homogeneous Electric Fields: Implementation of a Conjugate-Gradient Algorithm. *Phys. Rev. B* **1997**, *55*, 10337–10354.
46. Gonze, X.; Amadon, B.; Anglade, P. M.; Beuken, J. M.; Bottin, F.; Boulanger, P.; Bruneval, F.; Caliste, D.; Caracas, R.; Cote, M.; *et al.* ABINIT: First-Principles Approach to Material and Nanosystem Properties. *Comput. Phys. Commun.* **2009**, *180*, 2582–2615.
47. Gonze, X.; Rignanese, G. M.; Verstraete, M.; Beuken, J. M.; Pouillon, Y.; Caracas, R.; Jollet, F.; Torrent, M.; Zerah, G.; Mikami, M.; *et al.* A Brief Introduction to the ABINIT Software Package. *Z. Kristallogr.* **2005**, *220*, 558–562.
48. Savrasov, S. Y.; Savrasov, D. Y. Electron−Phonon Interactions and Related Physical Properties of Metals from Linear-Response Theory. *Phys. Rev. B* **1996**, *54*, 16487–16501.
49. Jansen, A. G. M.; Vangelder, A. P.; Wyder, P. Point-Contact Spectroscopy in Metals. *J. Phys. C* **1980**, *13*, 6073–6118.
50. Allen, P. B. The Electron−Phonon Coupling Constant Lambda. In *Handbook of Superconductivity*; Academic Press: New York, 1999.